



Technical Sciences
Academy of Romania
www.jesi.astr.ro

Received 13 May 2021

Accepted 14 September 2021

Received in revised form 9 August 2021

FEM analysis of Storz coupling

**GEORGE GHIOCEL OJOC¹, CORNEL BĂBUȚ²,
NICOLAE UNGUREANU², LORENA DELEANU^{1*}**

¹"Dunărea de Jos" University of Galati, Faculty of Science and Environment, 47
Domnească Street, RO-800008, Galati, Romania

²Technical University Cluj-Napoca, Romania

Abstract. This paper presents an isothermal model of Storz coupling used in fire hose coupling. The model has the actual geometry of the coupling Fire and Rescue NSW for the nominal diameter of 65 mm (NEN 3374). The simulation was done for a load interval on the coupling (from $F=2$ kN for an actual value of water pressure, to extreme conditions with $F=3$ kN and 6 kN when the coupling fails under load). The stress and strain distributions point out the stress concentrators and the maximum values of von Mises stress in order to compare them to the material limit. The coupling is made of aluminum alloy EN AW6082 (AlSi1MgMn), treatment T6 (solution heat treated, quenched and artificially aged). Bottom surface of one half-coupling is fixed and the upper surface of the other half-coupling is loaded with a tensile force, uniformly distributed on surface. The constitutive model of the material is bilinear with Young modulus of 71000 MPa, Poisson ration 0.33, yield limit of 280 MPa, ultimate tensile strength 310 MPa and plastic equivalent strain 0.14.

Keywords: FE analysis, stress and strain distribution, bilinear constitutive model.

1. Introduction

Storz couplings have a great resistance against corrosion, acids and water and are frequently used by firefighter. This is why they are also known as firefighting couplings or fire hose fittings [1]. Their resistance is dependent on the material which is why there are different materials available. Not only are these fire hose fittings excellent for working with water and other fluids, but Storz couplings are also able to connect hoses together [2], [3].

The simulation of mechanical behavior is useful because it could design limits of the input parameters (especially pressure) and could virtually investigate the

*Correspondence address: lorena.deleanu@ugal.ro

mechanical behavior, the actual tests being limited based on initial results obtained from simulation.

For firehoses, there are supra-pressures generated by the so-called “water hammer blow”, and the pressure difference is depending on the water velocity in nominal regime [4], [5], [6]:

$$\Delta p \cong 2 \dots 2.5 v_0 \quad (1)$$

where Δp is the over pressure in technical atmospheres, v_0 is the water velocity in nominal regime. It is recommended that water velocity is kept below 3 m/s [7], [8].

2. The model

When evaluating the behavior of a system, the methods may be analytical, mathematical or empirical based on experimental work. For complex shape systems, the method of finite element could give useful results if the model, the conditions and the mesh are adequate selected by users [9]

The usual operating pressure of a firehose may be between 8 and 16 bar (0.80 MPa and 1.6 MPa) [10]. Hose is one of the basic, essential pieces of fire-fighting equipment. It is necessary to convey water either from an open water supply, or pressurized water supply. Hoses are divided into two categories, based on their use: suction hose (designed to operate under negative pressure), and delivery or discharge hose (designed to operate under positive pressure). This last group include attack hose, supply hose, relay hose, forestry hose and booster hose. Attack hoses are fabric-covered, flexible hose used to bring water from the fire pumper to the nozzle, they hose range in nominal inside diameter from 38 mm to 76 mm) and are designed to operate at pressures up to about 2.76 MPa [11].

Hose connections are often made from brass, hardened aluminum alloy connections are also specified [7]. In countries using quick-action couplers for attack hoses, forged aluminum alloy has been used because the weight penalty of brass for Storz couplings is higher than for threaded connections.

The Storz coupling is frequently used for firehoses. It was invented by Carl August Guido Storz in 1882 and in 1890 it was patented in Switzerland and then, in 1893, in the USA. It was first specified in standard FEN 301-316, and has been used by German fire brigades since 1933. It is the standard coupling on firehoses in Austria, Denmark, Germany Portugal, Romania, Switzerland, Sweden, the Netherlands, Poland, Israel and Greece and it is also used in Australia and the USA [12].

The model consists of two half-coupling (Figure 1), attached as in actual functioning position. The applied force was on the top surface of the upper half-coupling and the bottom surface of the lower half-coupling was fixed. The simulation was done for $F=2$ kN, $F=3$ kN and $F=6$ kN in order to point out the failure of the hooks for higher load (3...6 kN).

The following steps were done for simulation:

- model drawing for a nominal diameter of 65 mm;
- mesh network with refined volume for the hooks (Fig. 2);

- constitutive model of the material based on EN 755-3 (Table 1);
- boundary conditions: the bottom surface of the inferior half coupling of the model is fixed;
- loading is applied uniformly on the upper surface of the upper half-coupling; the simulation was run for $F=2$ kN, 3 kN and 6 kN; load was applied in a ramp till its maximum value is applied at moment $t=1 \times 10^{-4}$ s; simulation was run for a time interval of 2.5×10^{-4} s, taking into consideration that maximum values for stress and strain become constant
- simulation was run in Explicit Dynamics (Ansys) and analysis was done for von Mises stress distributions and elastic, plastic and strains;
- friction was taken into account (COF=0.3, considered constant).

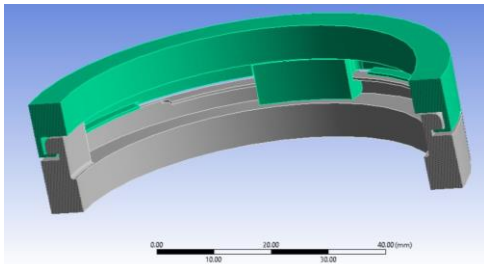


Fig. 1. Storz coupling, as analyzed in this study.

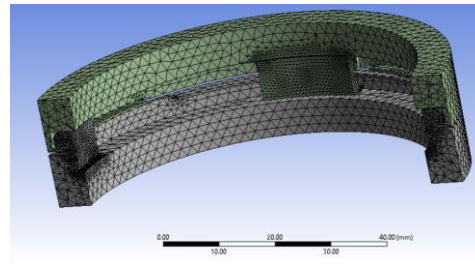


Fig. 2. Mesh detail.

In Romania, Storz couplings are made of aluminum alloy grade AlSi5Cu1Mg. Many producers also use for Storz couplings EN AW-6082 [13], [14] with the treatment T6, this one having better mechanical characteristics, including a good value for elongation at break.

The constitutive material model is a bilinear hardening model, having the yield stress 280 [MPa], the tensile limit 310 MPa, the elongation at break 0.14, Young modulus of 71000 MPa, Poisson ration 0.33, yield limit of 280 MPa, ultimate tensile strength 310 MPa and plastic equivalent strain 0.14.

Table 1. Mechanical characteristics for aluminum alloy

Treatment	Wall thickness, e [mm]	Yield stress [MPa]	Tensile limit [MPa]	Elongation at break [%]	Hardness HB
T4	$e \leq 25$	110	205	14	65
T5	$e \leq 5$	230	270	8	80
T6	$5 < e \leq 25$	260...280	310	10...14	95

Treatment designation according to EN 515: T4 – naturally aged to a stable condition, T5 – cooled from an elevated temperature forming operation and artificially aged, T6 – solution heat treated, press quenched and artificially aged; for different wall thickness within one profile, the lowest values shall be considered for all cross section.

3. Results

The simulation was run for three cases with different forces acting on the top surface of the upper half-coupling in order to analyze the von Mises stress and

strain distributions, to identify possible failure mechanisms. For $F=6$ kN, the values are increasing sharply after load is reaching the set value, the hook having integrity till $t=1.625 \times 10^{-4}$ s. The crack is starting at almost the middle of the hook length (Fig. 3) and it is propagating rapidly, at $t=2.5 \times 10^{-4}$ s, the hook is completely fragmented. Thus, this is not a load supported by the analyzed Storz coupling. For $F=3$ kN, the crack is initiated later, the hook is not cut off completely at the end of the simulation, at 2.5×10^{-4} s (Figs. 8-10). For $F=2$ kN, the coupling is kept without cracks and this is obvious because maximum values of von Mises stress are under the tensile limit.

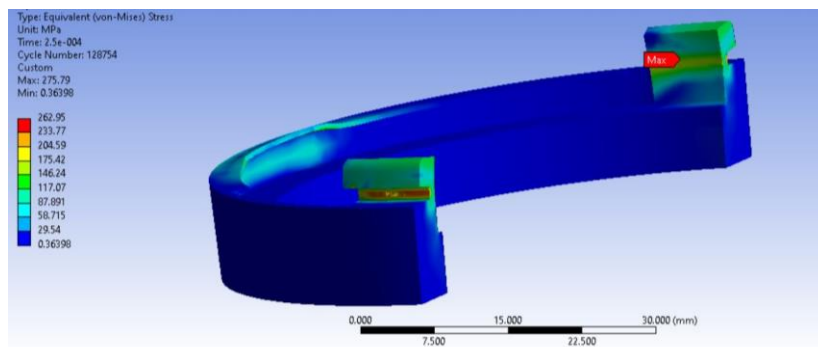


Fig. 3. View of the upper half-coupling with crack initiation in the middle of the hook length, in the thin cross section, at moment $t=1.625 \times 10^{-4}$ s, for $F=3$ kN.

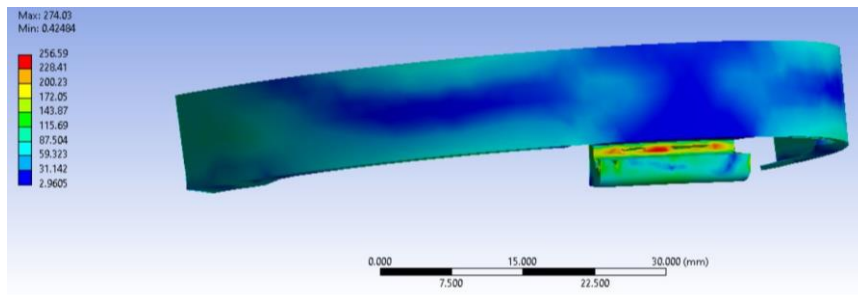


Fig. 4. View of the upper half-coupling with crack initiation in the middle of the hook length, in the thin cross section, at moment $t=1.625 \times 10^{-4}$ s, for $F=6$ kN.

Figure 5 presents the maximum values for von Mises stress during the simulation. For all simulations, the maximum values appear on the inner surface of the hooks. For simulated cases, the maximum values for elastic strain are almost the same at the end of the simulation (Fig. 6), meaning that the coupling is not working in the elastic domain of the material, but it exhibits plastic strain, too, the maximum values of the plastic strain being given in Fig. 7. When load increases, the plastic strain is present earlier. The critical equivalent plastic strain is reached for loads $F=3$ kN and $F=6$ kN.

The analyses in Explicit Dynamics allow for pointing out the stress concentrators that are important to be known in order to make the system to function safely [15].

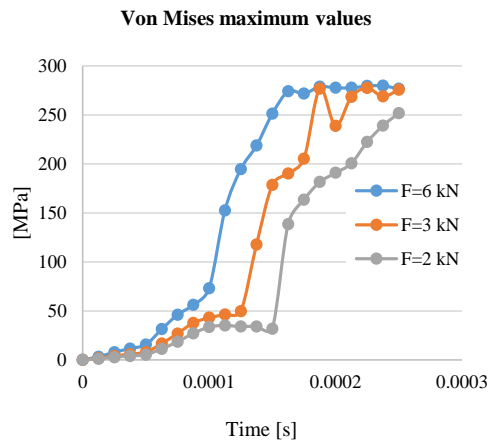


Fig. 5. Evolution in time of the maximum values of von Mises stress.

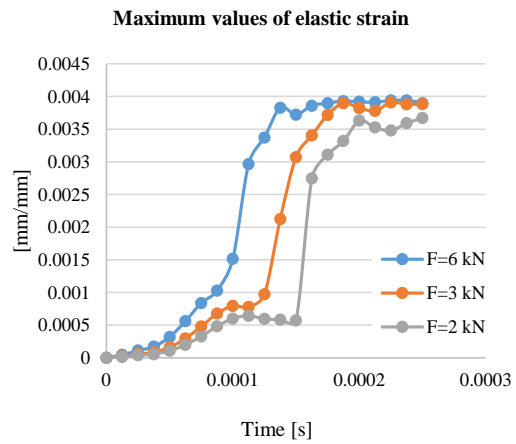


Fig. 6. Evolution in time of the maximum values of elastic strain.

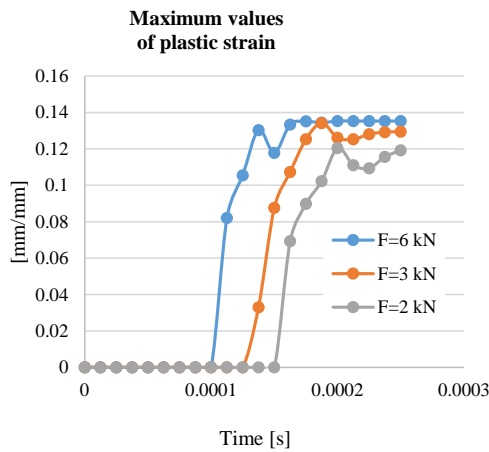


Fig. 7. Evolution in time of the maximum values of plastic strain.

For Storz couplings, stress concentrators are located in the zones with thin cross sections and at the edges of the contacting parts. For the geometry of the analyzed Storz coupling, the thickness and fillets are important in evaluating the equivalent stress values. For instance, the hook leg in Fig. 8 shows a large band of high values of von Mises stress (higher on the inner side, towards the bridle). Even at lower load of 2 kN, corresponding to an inner pressure of 6 bar, the maximum value of equivalent stress reaches 250 MPa, a value near the yield limit, being overpassed in the same region for higher loads (3 kN and 6 kN). Crack initiations are visible on the inner surface of the hook for these loads. The bridle is damaged near the contact with the hook, at 3 kN by plastic deformation, but at 6 kN, this element is also broken.

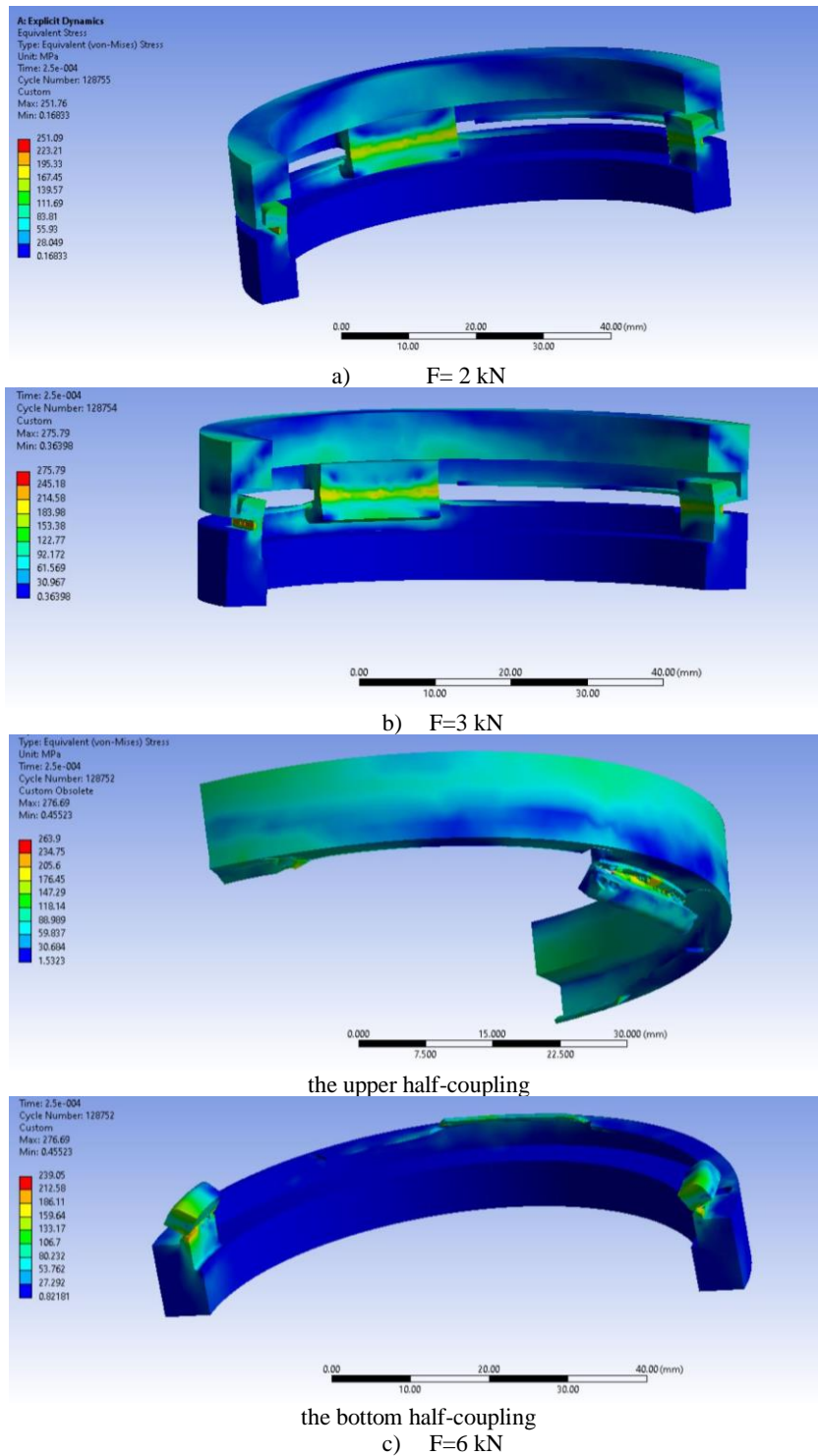


Fig. 8. von Mises stress distribution (in MPa) in Storz coupling, at moment $t=2.5 \times 10^{-4}$ s.

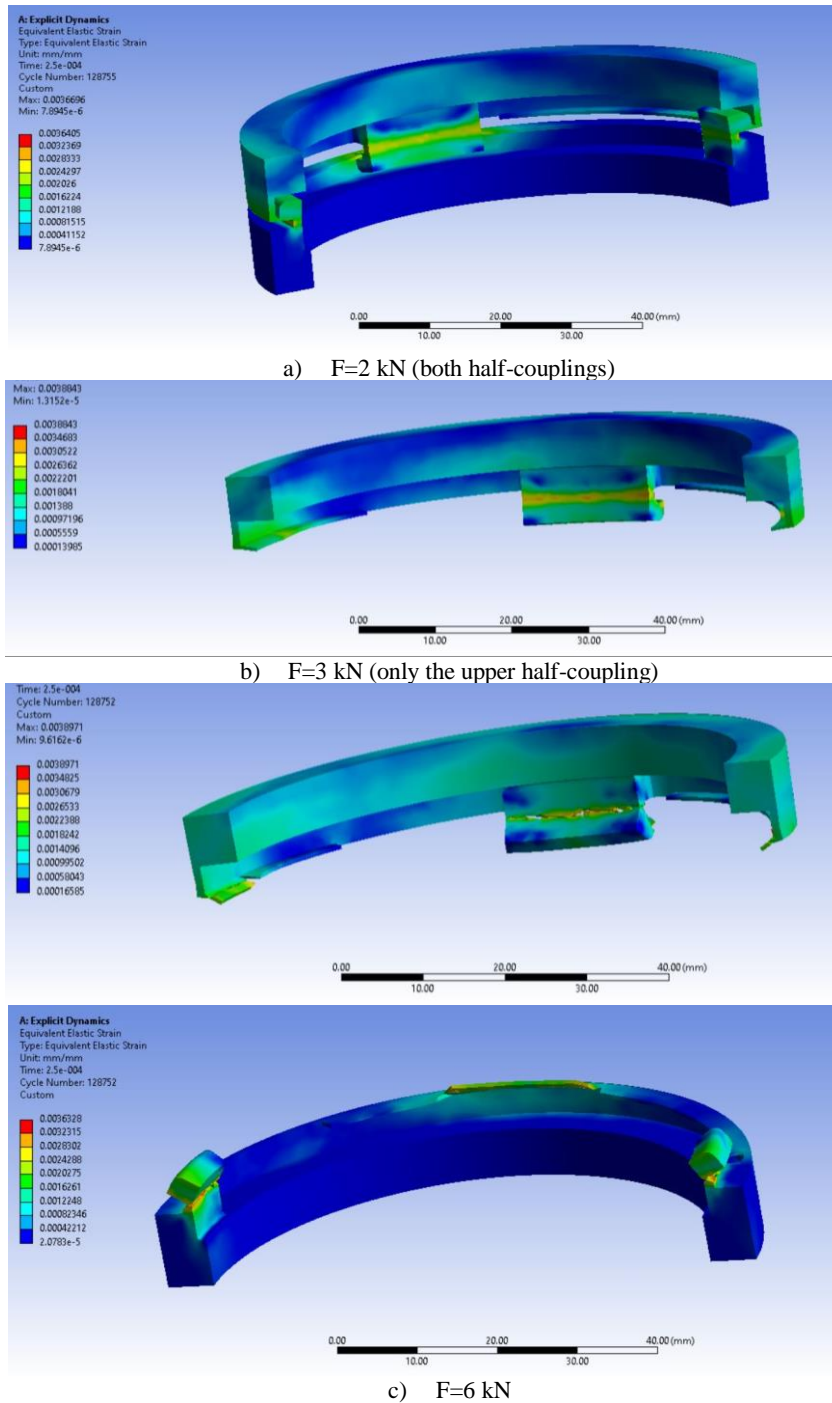


Fig. 9. von Mises stress distribution (in MPa) in Storz coupling, at moment $t=2.5 \times 10^{-4}$ s.

The circular bridle that fixed the hook is also damaged, just next to the hook contact and it is strongly deformed.

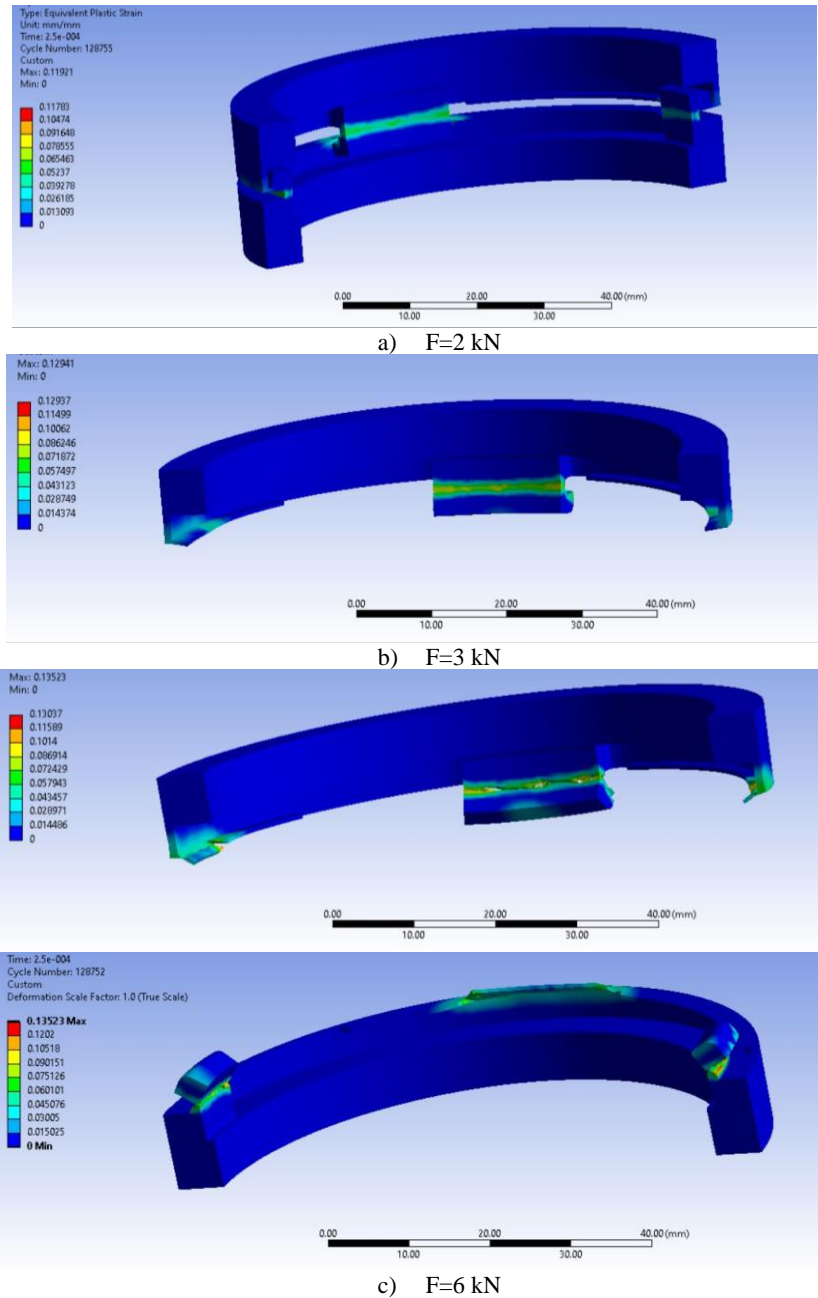
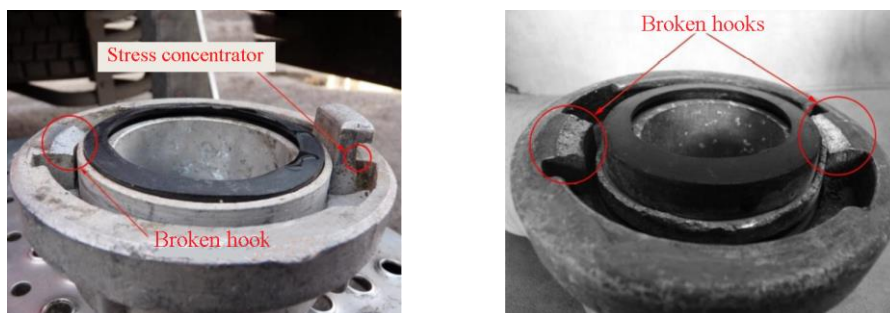


Fig. 10. The equivalent plastic strain distributions for the simulated cases, at moment $t=2.5 \times 10^{-4}$ s.

The plastic strain (Fig. 10) appears concentrated in the hook leg and the bridle under contact and near it. Values near EPS are obtained for 3 kN and 6 kN, preceding the break.

For $F=2$ kN, a load that could be maintain in actual coupling, the high values of plastic strain are located in the thinner section of the hook and in the bridle ends in contact.

The model is qualitatively validated by the failures presented and discussed in [16],[17] photographs in Figure 9, presenting the breakage of the hooks (also named lugs). In many cases in practice, only one hook is broken due to uneven distribution of load on the coupling, but the photo in Figure 9b is very similar to the virtual breakage obtained by simulation.



a) asymmetrical break of one hook and damage initiation on the other hook

b) both hooks on the half-coupling are broken

Fig. 11. Photos of failed half-couplings.

4. Conclusions

There are presented results of simulating the loading of a Storz coupling in order to evaluate how the coupling is failing and to establish a model for determining the limit of the coupling loading.

The authors used a bilinear hardening constitutive model for the material the coupling is made of with constants experimentally determined for the aluminum alloy EN AW-6082.

Analyzing von Mises stress distributions, the authors could identify the failure mechanisms and the aspect of the hook break, which are similar to the actual ones. The simulations pointed out stress concentrations in the thinner cross section of the hooks and in the contact edges of the thin bridle. These are the weaken zone of the coupling and a higher load could be sustained if these will be re-designed.

This simulation is useful for establishing initial limits for the upper pressure (and the force acting on the coupling) that can be used with this type of coupling. Also, the simulation could be run for different geometry of the hook and bridle and analyzing the results, the shape, fillets and other dimensions could be easier modified to evaluate the stress distribution and to improve the shape in order to

decrease the stress concentrators and the plastic strain, avoiding shape change and loss of tightness.

Acknowledgement

This paper was orally presented to the 9th edition of the Scientific Conference organized by the Doctoral Schools of “Dunărea de Jos” University of Galati (SCDS-UDJG) <http://www.cssd-udjg.ugal.ro/> that was held on 10th and 11th of June 2021, in Galati, Romania.

This work is supported by the project ANTREPRENORDOC, in the framework of Human Resources Development Operational Programme 2014-2020, financed from the European Social Fund under the contract number 36355/23.05.2019 HRD OP /380/6/13 – SMIS Code: 123847.

References

1. *** Fire hose, https://en.wikipedia.org/wiki/Fire_hose
2. Calotă, S. et al., *Manualul Pompierului*, Editura Imprimeriei de Vest, Oradea 2009
3. S. van der Veen, Everything you need to know about Storz couplings, <https://shop.eriks.nl/en/storz-couplings/>, accessed 30.05.2021
4. Bălulescu P., Crăciun I., *Agenda pompierului*, Editura Tehnică, București, 1993, p. 22
5. Răduleț, R., ș.a., *Lexiconul Tehnic Român*, ediția a doua, Editura Tehnică, Bucharest, 1957-1966
6. Dorf, R., C., *CRC Handbook of Engineering Tables*, CRC Press, Fl. U.S.A., 2003
7. Goldwater S. and R. F. Nelson. "Large-Diameter Super Aquaduct Flexible Pipeline Applications in the Fire Service." *Fire Engineering* (April 1997), p. 147-149
8. ****Manual pentru cunoașterea accesoriilor, utilajelor și autospecialelor de stingere a incendiilor*, Editura Ministerului de Interne, 1992
9. Năstăsescu V., Iliescu N., Marzavan S., Element-Free Galerkin Method and Finite Element Method. Which is better?, *Journal of Engineering Sciences and Innovation* Volume 5, Issue 4 / 2020, p. 287 – 298
10. *** Storz coupling, (accessed 1.08.2021) <https://www.flexible-hose-and-coupling-tecalemit.com/en/storz-couplings>
11. *** NFPA 1961: Fire Hose. National Fire Protection Association, 1997
12. *** Storz, <https://en.wikipedia.org/wiki/Storz>
13. *** Alloy Data Sheet EN AW-6082 [AlSi1MgMn], <https://www.nedal.com/wp-content/uploads/2016/11/Nedal-alloy-Datasheet-EN-AW-6082.pdf>
14. *SR-EN-1706 : 2010. Aluminiu și aliaje de aluminiu. Piese turnate. Compoziție chimică și caracteristici mecanice*, București, 2010
15. Barsanescu P. D., Iftimie N., Steigmann R., Dobrescu G. S., Danila N. A., Savin A., Damage detection of critical zones of wind turbine blades based on the complementary methods, *Journal of Engineering Sciences and Innovation* Volume 5, Issue 3 / 2020, pp. 197-204
16. Băbuț, C., *Raport de cercetare I - Fiabilitatea și mentenanța elementelor de cuplare a furtunurilor pentru instalațiile de stins incendii (in Romanian)*, Technical University of Cluj-Napoca, Centrul Universitar Nord Baia Mare, Școala Doctorală, 2016
17. Babut C., Ungureanu N., Ungureanu M., Research on fire hose couplings damages, *International Conference on Applied Sciences (ICAS2016)*, IOP Conf. Series: Materials Science and Engineering 163 (2017) 012016, doi:10.1088/1757-899X/163/1/012016